This full text paper was peer reviewed at the direction of IEEE Communications Society subject matter experts for publication in the ICC 2007 proceedings.

Analysis of Code-Assisted Blind Synchronization for UWB Systems

Yeqiu Ying[1], Mounir Ghogho[1] and Ananthram Swami[2]
[1] School of Electronic and Electrical Engineering
University of Leeds, LS29JT, UK
[2] ARL, Adelphi, MD, USA
Emails:{eenyyi, m.ghogho}@leeds.ac.uk
a.swami@ieee.org

***Abstract*— Timing synchronization is a preeminent challenge in ultra-wideband impulse radios (UWB-IRs). The conventional all-digital synchronization methods encounter some formidable implementation difficulties such as high rate sampling and high complexity RAKE structure. To avoid these challenges, semi-analog methods have been motivated recently. We have recently proposed a code-assisted blind synchronization (CABS) algorithm to realize timing synchronization blindly with the help of the discriminative property of both time hopping codes and well-designed polarity codes. The algorithm requires sampling at the frame rate only and bypasses channel estimation during the synchronization phase. This paper analyzes the identifiability and both the probability of acquisition and the the mean square error performance of CABS analytically. A data-aided code-assisted synchronization (CAS) algorithm is also proposed and a modified version of CABS which relies solely on the time hopping code is investigated.**

I. Introduction

Recently, ultra-wideband (UWB) radio has been attracting increasing interest due to its unique advantages such as precise ranging resolution, enhanced obstacle penetration capability, and low cost transceiver hardware (see [1] and references therein). All these unique advantages make UWB radio a good candidate for wireless applications such as location-aware communications and wireless sensor networks.

To realize the unique theoretical advantages of UWB, many physical and MAC layer problems have to be overcome. Timing synchronization is one of the most crucial issues since its accuracy has a great impact on system throughput, capacity and bit error rate [2][3][4][5]. Indeed, due to the transmission of low power and ultra-short duration pulses, timing synchronization is very challenging in UWB impulse radios (IRs), especially given the low complexity-low cost philosophy of UWB. Synchronization algorithms following an all-digital route have to cope with some prohibitive implementation hurdles such as the requirement of an extremely high speed analog-to-digital converter, estimation of a large number of channel parameters, and a RAKE receiver structure with a large number of fingers [6]. This motivates the research of designing low complexity semi-analog methods[7][8]. In [8] we proposed a code-assisted blind synchronization (CABS) algorithm based on the discriminative property of a well-designed polarity code and the time hopping (TH) code of the desired user. With the discriminative nature of both codes, the algorithm can achieve fast and accurate synchronization even in the presence of multi-user interference, while avoiding high rate sampling and bypassing challenging channel estimation.

The algorithm was validated by both intuitive explanation and numerical simulations in [8]. In this paper, we extend our work by providing an extensive analytical performance analysis. Identifiability is first analyzed. Then, for coarse symbol-level synchronization, we study the probability of acquisition, and a lower bound on this probability is derived in closed-form. The performance of fine synchronization is assessed using the mean squared error (MSE), and an upper bound on the asymptotic MSE (AMSE) is derived. We also propose a data-aided version of CABS, called code-assisted synchronization (CAS) that provides better performance than CABS. To relieve the challenging polarity code design in CABS, we investigate a modified version which relies on the TH code only, and compare its performance with the initial CABS algorithm by simulations.

This paper is organized as follows. Section II defines the models that describe the UWB signal and the propagation channel. In Section III we review the CABS algorithm and introduce the CAS algorithm. The identifiability of CABS is investigated in Section IV, followed by the analytical performance analysis in Section V. Numerical simulation results and discussions are given in Section VI. Finally we conclude our work in Section VII.

Notation: $\lfloor \cdot \rfloor$ stands for integer floor operation; $\langle \cdot \rangle_B$ denotes the modulo operator with base B, $\mathrm{E}\{\cdot\}$ and $\mathrm{var}\{\cdot\}$ represent the statistical expectation and variance operators, respectively.

II. System Model

In typical UWB-IRs, every information symbol is conveyed by a sequence of N_f pulses, $p(t)$, each with ultra short duration, T_p, of the order of nanosecond. During each frame of duration T_f, one data modulated pulse is transmitted, resulting in a symbol duration of $T_s = N_f T_f$. The two most popular modulation schemes used in UWB-IRs are binary pulse amplitude modulation (BPAM) and binary pulse position modulation (BPPM), which were compared in terms of performance and implementation complexity in [9][10]. Since BPAM outperforms BPPM in terms of bit error rate (BER), we focus on BPAM UWB here, and the extension

1-4244-0353-7/07/$25.00 ©2007 IEEE

Report Documentation Page

Form Approved
OMB No. 0704-0188

1. REPORT DATE	2. REPORT TYPE	3. DATES COVERED
JUN 2007		**00-00-2007 to 00-00-2007**

4. TITLE AND SUBTITLE	5a. CONTRACT NUMBER
Analysis of Code-Assisted Blind Synchronization for UWB Systems	5b. GRANT NUMBER
	5c. PROGRAM ELEMENT NUMBER
6. AUTHOR(S)	5d. PROJECT NUMBER
	5e. TASK NUMBER
	5f. WORK UNIT NUMBER
7. PERFORMING ORGANIZATION NAME(S) AND ADDRESS(ES) **Army Research Laboratory,Adelphi,MD,20783**	8. PERFORMING ORGANIZATION REPORT NUMBER
9. SPONSORING/MONITORING AGENCY NAME(S) AND ADDRESS(ES)	10. SPONSOR/MONITOR'S ACRONYM(S)
	11. SPONSOR/MONITOR'S REPORT NUMBER(S)

12. DISTRIBUTION/AVAILABILITY STATEMENT
Approved for public release; distribution unlimited

13. SUPPLEMENTARY NOTES
See also ADM002055. Proceedings of the 2007 IEEE International Conference of Communications (ICC 2007) Held in Glasgow, Scotland on June 24-28, 2007. U.S. Government or Federal Rights License

14. ABSTRACT
see report

15. SUBJECT TERMS

16. SECURITY CLASSIFICATION OF:			17. LIMITATION OF ABSTRACT	18. NUMBER OF PAGES	19a. NAME OF RESPONSIBLE PERSON
a. REPORT **unclassified**	b. ABSTRACT **unclassified**	c. THIS PAGE **unclassified**	**Same as Report (SAR)**	**6**	

of the results to BPPM UWB is straightforward. In order to smoothen the spectrum as well as to enable multiple access, periodic pseudo-random TH codes are used to time-shift the positions of the pulses by integer multiples of chip duration $T_c := \lfloor \frac{T_f}{N_c} \rfloor$, with N_c denoting the number of chips per frame within the associated frames. TH was shown to be a good spectrum smoothing and multiple access scheme [11], especially for the low data rate applications.

Therefore, in the conventional TH-UWB radios the pulses across the frames of each symbol have the same polarity. As pointed out in [8], the polarities of the pulses within each symbol can also be modified by making use of well-designed polarity codes to ease synchronization. Thus the transmitted signal in a point to point link can be expressed as

$$u(t) = \sum_{k=0}^{+\infty} a_k \sum_{i=0}^{N_f-1} d_i p(t - kT_s - iT_f - c_i T_c) \qquad (1)$$

where $\{a_k\}$'s are the BPAM information symbols taking values ± 1 with equal probability, $\{d_i\}_{i=0}^{N_f-1}$ is the bipolar representation of a binary code (i.e. $d_i = \pm 1$), and $\{c_i\}_{i=0}^{N_f-1}$ is the TH sequence whose elements are integer values randomly chosen from $[0, N_h - 1]$, where $N_h < N_c$. Note that if $d_i = 1,\ \forall i$, $u(t)$ reduces to the usual transmitted TH BPAM-UWB IR signal.

The signal $u(t)$ propagates through an L-path fading channel with $\{\gamma_l\}$ and $\{\tau_l\}$ representing the amplitude and the delay of the lth path, and without loss of generality we assume $\tau_0 < \tau_1 < ... < \tau_{L-1}$. The channel is also assumed to be quasi-stationary, i.e. $\{\gamma_l,\ \tau_l\}_{l=0}^{L}$ are invariant over a burst of several symbols. Therefore, the channel impulse response can be denoted by $h(t) = \sum_{l=0}^{L-1} \gamma_l \delta(t - \tau_l)$. The targeted timing information refers to the delay of the first arriving path τ_0. Thus, we isolate τ_0 from the channel impulse response and define the dispersed pulse as $g_(t) := \sum_{l=0}^{L-1} \gamma_l p(t - \tau_{l,0})$ with $\tau_{l,0} := \tau_l - \tau_0,\ \forall l \in [0, L-1]$ denoting the relative delay of the lth path to the first path. Therefore, the maximum dispersion of the pulse is $T_g = T_p + \tau_{L-1,0}$.

The signal at the output of the receive antenna can then be written as

$$r(t) = \underbrace{\sum_{k=0}^{+\infty} a_k \sum_{i=0}^{N_f-1} d_i g(t - kT_s - iT_f - c_i T_c - \tau_0)}_{s(t)} + w(t) \qquad (2)$$

where $s(t)$ represents the useful signal component and $w(t)$ accounts for the thermal noise which can be approximated as a wide sense stationary white Gaussian process with double-sided power spectral density $N_0/2$.

In this paper, we consider dense multipath propagation scenarios in which the channel paths are closely spaced. For analytical tractability we also assume $T_f > T_g + N_h T_c$ i.e. no inter-frame-interference (IFI), although CABS was shown by simulations in [8] to be robust against IFI.

III. Review of CABS Algorithm

CABS algorithm aims at estimating blindly the signal's propagation delay, τ_0, without channel state information. Blind synchronization algorithms are desired in many potential UWB radio applications such as wireless sensor and ad hoc networks where training may not be available. The complexity of estimating a large number of parameters of a typical UWB channel is prohibitive, thus bypassing channel estimation during the synchronization phase is desirable. The idea behind CABS is to rely on the discriminative property of both the polarity code and the TH code to adjust the candidate time shift until a maximum received signal energy is captured.

Since blind methods can only provide synchronization up to a symbol duration, we restrict τ_0 in the interval $[0,\ T_s)$. Then, the CABS algorithm can be expressed as the following optimization

$$\hat{\tau}_0 = \arg \max_{\tau \in [0, T_s)} J(\tau) \qquad (3)$$

with

$$J(\tau) = \frac{1}{K} \sum_{k'=1}^{K} \int_0^{T_I} \left| \sum_{j=0}^{N_f-1} d_j g_r(t) r(t + t_{k',j} + \tau) \right|^2 dt$$

where $t_{k',j} := k'T_s + jT_f + c_j T_c$, K is the number of symbol-long segments of the received waveform used for synchronization, $d_j g_r(t), t \in [0, T_f)$, with an effective support smaller than T_f, is the correlation template for the jth frame, and T_I is the integration interval. It is obvious that the shape of $d_j g_r(t)$ and the value of T_I affect the amount of the signal energy and the noise energy which are captured by each integration output, and thus affect the estimation accuracy. For simplicity of both implementation and analysis, we choose $d_j g_r(t)$ as a non-return-to-zero gate (NRZG) with polarity decided by d_j, i.e. $d_j g_r(t) = d_j, t \in [0, T_f]$. The optimization of T_I is dependent on the actual channel and the operating signal-to-noise ratio (SNR) value, and thus analytically untractable. If the receiver has the knowledge of the exact maximum channel delay spread, T_I can be set as T_g. Otherwise, T_I can be set to an upper bound of the maximum pulse dispersion $\bar{T}_g$, or even to $T_f - N_h T_c$.

It is worth pointing out that if training is allowed, a data-aided version of CABS (a.k.a. CAS), which can further improve the performance, is also feasible. By transmitting a training sequence with pattern of $a_k = (-1)^k$, CAS can be formulated as

$$\hat{\tau}_0 = \arg \max_{\tau \in [0, T_s)} J_{CAS}(\tau) \qquad (4)$$

with

$$J_{CAS}(\tau) = \int_0^{T_I} \left| \sum_{j=0}^{N_f-1} d_j g_r(t) \bar{r}(t + jT_f + c_j T_c) \right|^2 dt$$

where $\bar{r}(t) := \frac{1}{K} \sum_{k'=1}^{K} (-1)^{k'} r(t + kT_s + \tau),\ t \in [0, T_s]$ is a symbol-long segment of the averaged received waveform. Although analytical analysis for CAS is possible, in this paper

we only focus on CABS; extensions of these results to CAS can be obtained using the same reasoning.

IV. Identifiability Analysis for CABS

In [8], the validity of CABS was verified via an intuitive illustration and numerical simulations, and in this section we provide an analytical verification of the identifiability of CABS. Since the analysis when the pseudo random TH code is included is untractable, to simplify the noise-free part of the objective function, we assume $\{c_j\}_{j=0}^{N_f-1}$. For analytical simplicity, we also assume $T_I = T_g$; the ambiguity introduced by choosing $T_I \neq T_g$ will be discussed later on.

Therefore, the objective function given in (3) can be split into three terms by substituting $r(t)$ by (2)

$$J(\tau) = J_s(\tau) + J_{n_1}(\tau) + J_{n_2}(\tau), \tag{5}$$

where

$$J_s(\tau) = \frac{1}{K}\sum_{k'=1}^{K}\int_0^{T_g}\left|\sum_{j=0}^{N_f-1} d_j s(t+k'T_s+jT_f+\tau)\right|^2 dt, \tag{6}$$

$$\begin{aligned} J_{n_1}(\tau) &= \frac{2}{K}\sum_{k'=1}^{K}\int_0^{T_g}\sum_{j_1=0}^{N_f-1} d_{j_1} s(t+k'T_s+j_1T_f+\tau) \\ &\quad\times\sum_{j_2=0}^{N_f-1} d_{j_2} w(t+k'T_s+j_2T_f+\tau)dt \end{aligned} \tag{7}$$

and

$$J_{n_2}(\tau) = \frac{1}{K}\sum_{k'=1}^{K}\int_0^{T_g}\left|\sum_{j=0}^{N_f-1} d_j w(t+k'T_s+jT_f+\tau)\right|^2 dt. \tag{8}$$

Since the time delay τ_0 and the candidate time-shift τ are both within the range of $[0, T_s)$, the relative misalignment between them is $\tau - \tau_0 \in (-T_s, T_s)$. For clarity of exposition, we consider two cases: $\tau \leq \tau_0$ and $\tau \geq \tau_0$, separately. Under each case, we show that the noise-free term $J_s(\tau)$ is maximized if and only if (iff) $\tau = \tau_0$, which verifies the identifiability of CABS algorithm.

A. $\tau \leq \tau_0$

In this case, the relative misalignment between τ_0 and τ can be denoted as $\tilde{\tau}_0 := \tau_0 - \tau$, with $\tilde{\tau}_0 \in [0, T_s)$, and can be split into a frame-level misalignment quantity and a sub-frame-level misalignment quantity as: $\tilde{n}_0 = \lfloor \frac{\tilde{\tau}_0}{T_f} \rfloor$, $\tilde{n}_0 \in [0, N_f - 1]$, and $\tilde{\epsilon}_0 = \tilde{\tau}_0 - \tilde{n}_0 T_f$, $\tilde{\epsilon}_0 \in [0, T_f)$. After some manipulations and algebra, $J_s(\tau)$ can be simplified to:

$$\begin{aligned} J_s(\tau) &= \frac{N_f^2}{K}\sum_{k'=1}^{K}\left[R_d^2[-\tilde{n}_0; k']\int_0^{T_g} g^2(t-\tilde{\epsilon}_0)dt\right. \\ &\quad\left. + R_d^2[-\tilde{n}_0-1; k']\int_0^{T_g} g^2(t+T_f-\tilde{\epsilon}_0)dt\right], \end{aligned} \tag{9}$$

where $R_d[n; k'] := \frac{1}{N_f}\sum_{j=0}^{N_f-1} d_j d_{\langle j+n\rangle_{N_f}} a_{k'+\lfloor \frac{j+n}{N_f}\rfloor}$. If the two consecutive BPAM symbols $a_{k'}$ and $a_{k'+\lfloor \frac{j+n}{N_f}\rfloor}$ are the same, $R_d[n; k'] = R_d^+[n] := \frac{1}{N_f}\sum_{j=0}^{N_f-1} d_j d_{\langle j+n\rangle_{N_f}}$. Otherwise, $R_d[n; k'] = R_d^-[n] := \frac{1}{N_f}\sum_{j=0}^{N_f-1} d_j d_{\langle j+n\rangle_{N_f}^-}$ where $\langle n\rangle_N^- = (-1)^{\lfloor n/N\rfloor}\langle n\rangle_N$. Since $\tilde{n}_0 \in [0, N_f - 1]$ and $\tilde{\epsilon}_0 \in [0, T_f)$, it is obvious that $J_s(\tau|\tau \leq \tau_0)$ is maximized iff $\tilde{n}_0 = 0$ and $\tilde{\epsilon}_0 = 0$, i.e. $\tau = \tau_0$, and the maximum equals $N_f^2 E_g$ where $E_g := \int_0^{T_g} g^2(t)dt$ is the energy of each channel-dispersed pulse.

B. $\tau \geq \tau_0$

The relative misalignment, in this case, can be denoted as $\tilde{\tau}_0 := \tau - \tau_0$. Keeping the definitions for the other parameters involved the same as those in the above case, and following a similar derivation, we obtain:

$$\begin{aligned} J_s(\tau) &= \frac{N_f^2}{K}\sum_{k'=1}^{K}\left[R_d^2[\tilde{n}_0; k']\int_0^{T_g} g^2(t+\tilde{\epsilon}_0)dt\right. \\ &\quad\left. + R_d^2[\tilde{n}_0+1; k']\int_0^{T_g} g^2(t-T_f+\tilde{\epsilon}_0)dt\right], \end{aligned} \tag{10}$$

and with the same arguments made in the first case we can conclude that $J_s(\tau|\tau \geq \tau_0)$ reaches its maximum $N_f^2 E_g$ iff $\tilde{n}_0 = 0$ and $\tilde{\epsilon}_0 = 0$, i.e. $\tau = \tau_0$.

Combining these two cases together, the CABS algorithm proposed in (3) can be corroborated identifiable if T_g is known. In practice, however, the exact value of T_g is unavailable at the receiver. In this case, the value of T_I can be set as either $\bar{T}_g$ or a value which is smaller than T_g. If $T_I > T_g$, an uncertainty area of $[-(T_I - T_g) + \tau_0, \tau_0]$ exists, and if $T_I < T_g$, the uncertainty area depends on the actual channel delay profile.

V. Performance Analysis

A. Probability of Acquisition

In UWB IRs, coarse timing acquisition aims at finding the boundaries between symbols in the received waveform. In fact, the autocorrelation-based detection schemes such as transmitted reference (TR) [12], and differentiate decoding (DIFF) [13] are more sensitive to the frame-level timing mismatch [14] than the sub-frame timing mismatch. Therefore, the probability of acquiring the coarse timing synchronization is more of interest than the exact MSE of the delay estimate for autocorrelation based receivers. Here we derive the lower bounds on the probability of acquisition of CABS for the coarse timing acquisition.

During the coarse timing synchronization, N_f candidate time offsets $\tau = nT_f$ with integer $n \in [0,\ N_f - 1]$ are tested, which is the same as setting the search step $T_\triangle = T_f$. If the synchronizer can lock the receiver onto a candidate offset that is closest to the actual delay, we then say that coarse acquisition is achieved. This coarse acquisition problem can then be formulated as estimating n_0 by the following optimization

$$\hat{n}_0 = \arg\max_{n=0\ldots N_f-1} J(nT_f),$$

so that $|\tau_0 - n_0 T_f| < \frac{T_f}{2}$. The probability of acquisition can be defined as:

$$\begin{aligned} P_a(n_0) &= \Pr\{\hat{n}_0 = n_0\} \\ &= 1 - \Pr\left\{ \bigcup_{n \neq n_0} J(nT_f) > J(n_0 T_f) \right\} \end{aligned} \quad (11)$$

or

$$\begin{aligned} P_a(n_0) = \int_{-\infty}^{+\infty} f_{n_0}(x_0) \Big(\int \cdots \int_{-\infty}^{x_0} \\ \times f_{n \neq n_0}(x_1, \ldots, x_{N_f - 1}) dx_1 \cdots dx_{N_f - 1} \Big) dx_0 \end{aligned} \quad (12)$$

where $\bigcup$ stands for the union of sets, $f_{n_0}(x)$ is the probability density function (*pdf*) of the random variable $J(n_0 T_f)$ and $f_{n \neq n_0}(x_1, \ldots, dx_{N_f - 1})$ is the joint *pdf* of the random variables $J(nT_f),\ n \in [0, N_f - 1]$, and $n \neq n_0$. Using the central limit theorem, $J(nT_f),\ n = 0 \ldots N_f - 1$ can be modeled as Gaussian random variables. For analytical tractability, we assume they are independent to each other, although the independence of these random variables is not actually valid due to the long channel delay spread and the overlap among the observation windows. We also assume that $\tilde{\epsilon}_0 = 0$ to simplify the derivation.

The first lower bound on P_a is derived based on Bonferroni Inequality [15] and is referred to as the 'Union Lower Bound' ($\underline{P}_{UB}$). Denoting $Y_n := J(nT_f) - J(n_0 T_f), n \neq n_0$, and with the Gaussian assumption on $J(nT_f)$, the Y_n's are also Gaussian random variables with mean m_{Y_n} and variance $\sigma^2_{Y_n}$). The Bonferroni Inequality states that for a countable set of events: $A_1, \ldots, A_N$, $\Pr\{\bigcup_i A_i\} \leq \sum_i \Pr\{A_i\}$ where the equality holds iff these events are mutually exclusive (or independent). Substituting Y_n into (11) and invoking the Bonferroni Inequality, we obtain:

$$P_a(n_0) \geq \underline{P}_{UB} = 1 - \sum_{n \neq n_0} Q\left\{ \frac{-m_{Y_n}}{\sqrt{\sigma^2_{Y_n}}} \right\}, \quad (13)$$

where $Q(x) = \frac{1}{2}\left(1 - \mathrm{erf}\left(\frac{x}{\sqrt{2}}\right)\right)$, with $\mathrm{erf}(x) = \frac{2}{\sqrt{\pi}} \int_0^x e^{-(t^2)} dt$ denoting the error function.

Since the $J(nT_f)$ are assumed independent and $\tilde{\epsilon}_0 = 0$, the mean and the variance of Y_n can be readily derived as:

$$m_{Y_n} = N_f^2 E_g \left(\frac{\left|R_d^+[+\tilde{n}_0]\right|^2 - \left|R_d^-[-\tilde{n}_0]\right|^2}{2} - 1 \right) \quad (14)$$

and

$$\begin{aligned} \sigma^2_{Y_n} &= \frac{N_f^4 E_g^2}{8K} \left(\left|R_d^+[-\tilde{n}_0]\right|^2 - \left|R_d^-[-\tilde{n}_0]\right|^2 \right)^2 \\ &+ \frac{(2K-1)\left|R_d^+[-\tilde{n}_0]\right|^2}{K^2} \sigma_w^2 \\ &+ \frac{\left|R_d^-[-\tilde{n}_0]\right|^2 + 2K}{K^2} \sigma_w^2 + \frac{2N_f^2 T_g}{K} \sigma_w^4 \end{aligned} \quad (15)$$

where $\tilde{n}_0 := n - n_0$. Noticing that, due to the periodic property of $R_d^+[j]$ and $R_d^-[j]$, we have that $\left|R_d^+[j]\right| = \left|R_d^+[j + N_f]\right|$ and $\left|R_d^-[j]\right| = \left|R_d^-[j + N_f]\right|$ and thus in (13) the summation over $\forall n \in [0, N_f - 1]$ and $n \neq n_0$ is equivalent to the summation over $-\tilde{n}_0 \in [1, N_f - 1]$.

Since it is well known that this $\underline{P}_{UB}$ derived based on the Bonferroni Inequality is very loose, we resort to the Jensen's Inequality instead, and derive another lower bound which is named Jensen Lower Bound ($\underline{P}_{JB}$). With the assumption of independence, the $(N_f - 1)-$fold joint probability distribution in (12) can be written as the product of the probability distribution of each random variable, and (23) can be modified as

$$P_a(n_0) = \int_{-\infty}^{+\infty} f_{n_0}(x_0) \left(\prod_{n \neq n_0} \int_{-\infty}^{x_0} f_n(x_n) dx_n \right) dx_0.$$

Applying the Jensen's Inequality, we obtain that

$$\begin{aligned} P_a(n_0) &= \int_{-\infty}^{+\infty} f_{n_0}(x_0) \left(\prod_{\substack{n=0 \\ n \neq n_0}}^{N_f - 1} \int_{-\infty}^{x_0} f_n(x_n) dx_n \right) dx_0 \\ &\geq \prod_{\substack{n=0 \\ n \neq n_0}}^{N_f - 1} \int_{-\infty}^{+\infty} f_{n_0}(x_0) \int_{-\infty}^{x_0} f_n(x_n) dx_n dx_0 \\ &= \prod_{-\tilde{n}_0 \in [1, N_f - 1]} Q\left(\frac{m_{Y_n}}{\sqrt{\sigma^2_{Y_n}}} \right) = \underline{P}_{JB}. \end{aligned} \quad (16)$$

B. Asymptotic MSE

Since $J(\tau)$ is a nonlinear function of τ, the finite-sample MSE analysis of $\hat{\tau}_0$ is extremely complicated. However, with sufficiently large SNR and/or K, a closed form upper bound on the MSE can be derived. Due to the page limitation, the details of the derivation are omitted here (see [16]), and the upper bound can be expressed as

$$\begin{aligned} \mathrm{E}\left\{\tilde{\tau}_0^2\right\} &= \Pr(\tilde{\tau}_0 \in [0, \xi]) \mathrm{E}\left\{\tilde{\tau}_0^2 | \tilde{\tau}_0 \in [0, \xi]\right\} \\ &+ \Pr(\tilde{\tau}_0 \in [-\xi, 0]) \mathrm{E}\left\{\tilde{\tau}_0^2 | \tilde{\tau}_0 \in [-\xi, 0]\right\} \\ &\leq \frac{\sigma_w^4}{K N_f^2 \min\{g^2(\xi)\dot{g}^2(\xi), g^2(T_g - \xi)\dot{g}^2(T_g - \xi)\}} \end{aligned} \quad (17)$$

where $\tilde{\tau}_0 := \hat{\tau}_0 - \tau_0,\ \tilde{\tau}_0 \in [0, \xi]$, and $\xi < T_p$ is a small positive scalar. This reveals that the MSE of $\hat{\tau}_0$ converges to zero as $K \to \infty$ and/or $\mathrm{SNR} \to \infty$. It is worth pointing out that to reach (17), or in other words to achieve the convergence of the MSE of $\hat{\tau}_0$, a specific shape of the elementary pulse $p(t)$ is required. However, conventional pulses such as the second derivative of a Gaussian pulse which is used in the ensuing simulations also enable CABS to realize accurate estimate of τ_0.

VI. Simulations and Discussions

In this section, we verify our analysis by numerical simulations. In all the ensuing simulations, $p(t)$ is chosen as the second derivative of a Gaussian pulse i.e. $p(t) = \sqrt{E_p}[1 - 4\pi(\frac{t-0.5}{\tau_p})^2] \exp\{-2\pi(\frac{t-0.5}{\tau_p})^2\}$, where $\tau_p = 0.4ns$ is the delay parameter of the pulse. The energy of this pulse is

normalized to unity, i.e. $E_p = 1$. Each symbol consists of $N_f = 13$ frames with frame duration $T_f = 60ns$. Each frame is composed of $N_c = 30$ chips and the chip duration is $T_c = \lfloor \frac{T_f}{N_c} \rfloor = 2ns$. The user specific TH codes are generated by randomly taking integer values from the range of $[0, N_h - 1]$ with $N_h = 16$, and the codes are periodic with period N_f. The binary polarity code we used is the same as the one we used in [8]. The multipath channel model simulated is 'CM1' from the IEEE 802.15 working group [17] with maximum excess delay of $39ns$, and normalized unity energy. When evaluating the normalized (with respect to T_s^2) MSE (NMSE), we set the interval of each discrete time bin to be $T_\Delta = \lfloor \frac{T_f}{N_\Delta} \rfloor = 4ns$ where $N_\Delta = 15$ is the number of grid search per frame. To evaluate the coarse acquisition performance of CABS, the time interval between two consecutive discrete search is $T_\Delta = T_f = 60ns$, i.e. $N_\Delta = 1$.

In the above sections, we assumed the pulses are not time-shifted by the TH code in order to make the analytical derivations tractable. In this section, we first show by simulations that the performance of CABS when TH is adopted is consistent to that when TH is absent. The NMSE and P_a of both cases are plotted versus E_p/N_o in Fig.1 and Fig.2, respectively. It can be seen that the two schemes have very similar performance. Therefore the analytical results obtained can also be used to evaluate the performance of CABS when TH is adopted. In Fig.2, the lower bounds of P_a derived in Section V are also shown. As expected, compared with $\underline{P}_{UB}$, $\underline{P}_{JB}$ is tight especially at low and medium SNR values, and can be used to analytically predict the acquisition performance of CABS.

We then compare the NMSE of CABS with that of CAS in Fig. 3. CAS offers higher estimation accuracy than CABS especially at low SNR values, and medium to large values of K. Thanks to the special training pattern, extra averaging of the analog signal is possible before the integration for CAS, which further eliminates the noise. The price paid for achieving this performance gain, however, is some extra analog delay lines and the loss of data rate to enable training sequence transmission.

In practice, the synchronizer has no knowledge about the starting time of each frame during the coarse acquisition stage, and the time positions at which $J(\tau)$ is evaluated can be anywhere within each frame, i.e. $\tilde{\epsilon}_0 = 0$ does not hold true in general. In this case, the definition of acquiring the coarse timing synchronization given in the previous sections needs to be modified. In fact, if the synchronizer can lock the receiver onto the time whose difference to the actual start of each symbol is smaller than one frame, i.e. $|\hat{\tau}_0 - \tau_0| < T_f$, the coarse timing acquisition is considered successful. Fig.4 illustrates the probability of $\hat{\tau}_0 \in (\tau_0 - T_f, \tau_0 + T_f)$ when CABS algorithm is exploited for coarse timing synchronization with $\tilde{\epsilon}_0 \in [0, T_f)$.

Since one of the gists of CABS algorithm is the symbol-periodic repetitive time position pattern of the received waveform, we are motivated to investigate a modified version of CABS which requires no need for the polarity code. Fig.5 and Fig.6 show the comparison of performance between the original and the modified CABS. Surprisingly, the two have almost identical NMSE. The coarse acquisition performance of the modified CABS is slightly degraded by removing the polarity code. This is intuitively explainable. The NMSE predicts the performance of the synchronizer during the fine timing synchronization stage, and the probability of acquisition reflects the performance of the synchronizer during the coarse timing synchronization stage. When the coarse timing acquisition is achieved, the discriminative effect of the polarity code disappears during the fine synchronization phase. However, the polarity code does affect the coarse timing performance of CABS. With this exposition, the challenge of designing good polarity codes is relieved and CABS can be enabled for conventional TH-UWB systems. However, if the TH code has the property that there exists any shifted version of the TH code which is identical to the code itself, there will be ambiguity. Nevertheless, the chance for the TH code to have such property is very small since the value of N_f is usually several tens or hundreds.

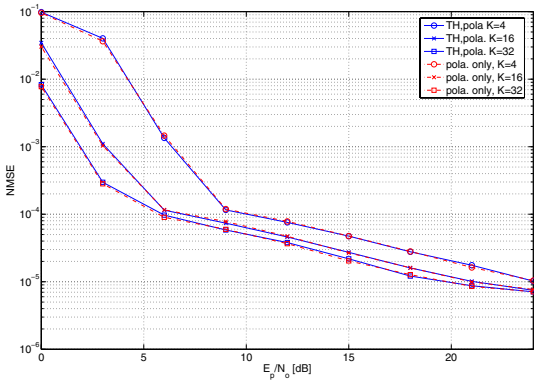

Fig. 1: NMSE of CABS with TH vs. without TH

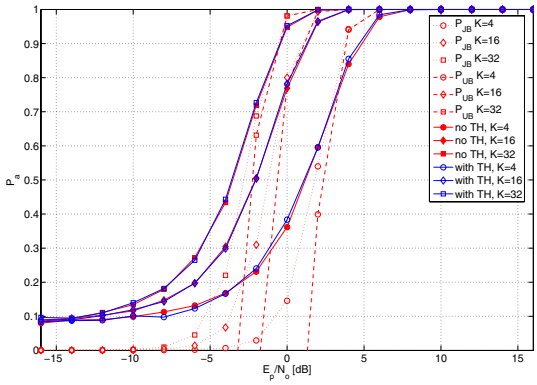

Fig. 2: P_a of CABS with TH vs. without TH

VII. Conclusions

In this paper, we extended our work on CABS algorithm which was initially proposed in [8] by providing an extensive analysis. We analytically verified the identifiability of CABS, and evaluated the asymptotic MSE and probability of acquisition during the coarse timing synchronization stage.

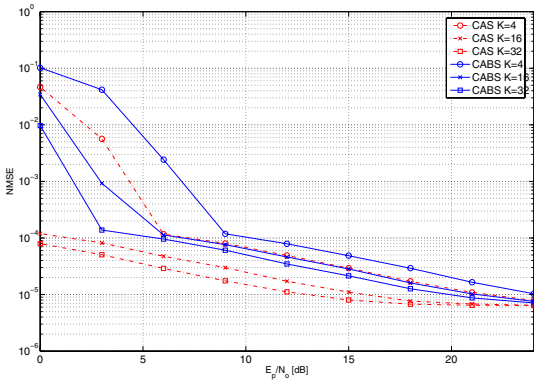

Fig. 3: NMSE comparison between CABS and CAS

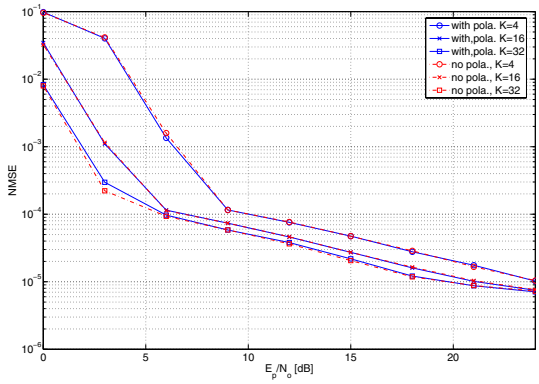

Fig. 5: NMSE of CABS with pola. vs. without pola. codes

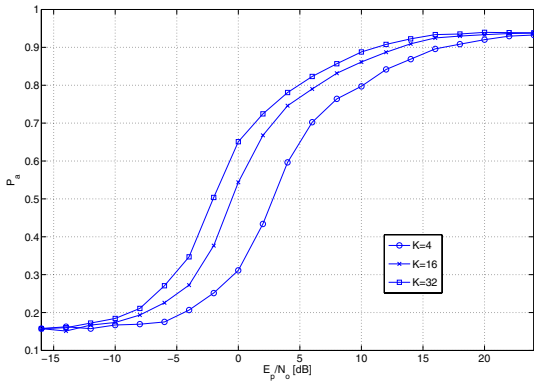

Fig. 4: Probability of acquisition with sub-frame misalignment

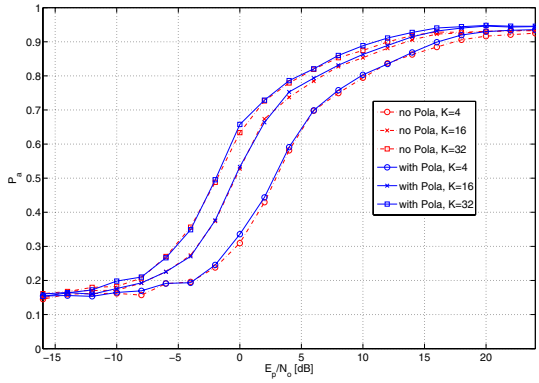

Fig. 6: Probability of acquisition with sub-frame misalignment,with/without pola. code

A data-aided version of code-assisted synchronization (CAS) algorithm which outperforms CABS was also proposed. To relieve the polarity code design challenge and to enable CABS in a conventional TH-UWB system, we also investigated a modified version of CABS which requires no polarity code.

REFERENCES

[1] Liuqing Yang and G. B. Giannakis, "Ultra-wideband communications: An idea whose time has come," *IEEE Signal Processing Magazine*, vol. 21, no. 6, pp. 26–54, November 2004.

[2] W. M. Lovelace and J. K. Townsend, "The Effects of Timing Jitter and Tracking on the Performance of Impulse Radio," *IEEE Journal on Selected Areas in Communications*, vol. 20, no. 9, pp. 1646–1651, December 2002.

[3] Dana Porrat and D. N. C. Tse, "Bandwidth Scaling in Ultra Wideband Communication," in *Proc. of 41st Allerton Conf. Univ. of Illinois at U-C*, Monticello IL, 1-3 October 2003.

[4] Zhi Tian and G. B. Giannakis, "BER sensitivity to mistiming in ultra-wideband impulse radios, Part I: Nonrandom channels," *IEEE Transactions on Signal Processing*, vol. 53, no. 4, pp. 1550 – 1560, April 2005.

[5] ——, "BER Sensitivity to Mistiming in Ultra-Wideband Impulse Radios Part II: Fading channels," *IEEE Transactions on Signal Processing*, vol. 53, no. 5, pp. 1897 – 1907, May 2005.

[6] Moe Z. Win and Robert A. Scholtz, "On the Energy Capture of Ultrawide Bandwidth Signals in dense multipath Environments," *IEEE Communications Letters*, vol. 2, no. 9, pp. 245–247, September 1998.

[7] Liuqing Yang and G. B. Giannakis, "Timing Ultra-Wideband Signals with Dirty Templates," *IEEE Transactions on Communications*, vol. 53, no. 11, November 2005. [Online]. Available: http://www.yang.ece.ufl.edu/publist.htm

[8] Mounir Ghogho and Yeqiu Ying, "Code-Assisted Blind Synchronization for UWB Systems," in *Proc. IEEE ICC'06*, Istambul, Turkey, June 2006.

[9] I. Guvenc and H. Arslan, "On the modulation options for UWB systems," in *Military Communications Conference, 2003. MILCOM 2003. IEEE*, vol. 2, 13-16 Oct. 2003, pp. 892–897Vol.2.

[10] G. Durisi and S. Benedetto, "Performance evaluation and comparison of different modulation schemes for UWB multiaccess systems," in *Communications, 2003. ICC '03. IEEE International Conference on*, vol. 3, 11-15 May 2003, pp. 2187–2191vol.3.

[11] M. Win and R. Scholtz, "Ultra-wide bandwidth time-hopping spread-spectrum impulse radio for wireless multiple-access communications," *Communications, IEEE Transactions on*, vol. 48, no. 4, pp. 679–689, April 2000.

[12] R. Hoctor and H. Tomlinson, "Delay-hopped transmitted-reference RF communications," in *Ultra Wideband Systems and Technologies, 2002. Digest of Papers. 2002 IEEE Conference on*, 21-23 May 2002, pp. 265–269.

[13] M. Ho, V. Somayazulu, J. Foerster, and S. Roy, "A Differential Detector for an Ultra-Wideband Communication System," in *Proc. IEEE VTC'02*, vol. 4, 6-9 May 2002, pp. 1896–1900.

[14] Ning He and Cihan Tepedelenlioglu, "Performance Analysis of Non-coherent UWB Receivers at Different Synchronization levels," in *Proc. IEEE GLOBECOM'04*, vol. 9, 29 November - 3 December 2004, pp. 3517–3521. [Online]. Available: http://www.eas.asu.edu/ cihan/papers.htm

[15] J. Proakis, *Digital Communications*, 4th ed. McGraw-Hill, New York, 2001.

[16] Yeqiu Ying, Mounir Ghogho, and Ananthram Swami, "Code-Assisted Synchronization for UWB Systems: Algorithms and Performance Analysis," *IEEE Transactions on Signal Processing*, (submitted).

[17] I. P. Working group for WPANs, *Channel Modeling Sub-committee Report Final*, November 2002.